Sequential local FRI sampling of infinite streams of Diracs

Jon Oñativia, Jose Antonio Urigüen and Pier Luigi Dragotti

Imperial College London

ICASSP 2013, Vancouver (Canada)

May 30, 2013

Outline

Sampling Finite Rate of Innovation Signals
- Signals with Finite Rate of Innovation
- Sampling process

Sequential algorithm
- Sampling an infinite sequence of Diracs
- The noisy scenario
- Application: neural activity detection

Signals with Finite Rate of Innovation (FRI)

- Signals that have a finite number of free parameters

$$x(t) = \sum_{k\in\mathbb{Z}} \sum_{r=0}^{R-1} a_{k,r}\, g_r(t - t_k).$$

If the set of functions $\{g_r(t)\}_{r=0,1,\ldots,R-1}$ is known, the signal $x(t)$ is perfectly determined by the coefficients $(a_{k,r}, t_k)$.

Signals with Finite Rate of Innovation (FRI)

- Signals that have a finite number of free parameters

$$x(t) = \sum_{k\in\mathbb{Z}} \sum_{r=0}^{R-1} a_{k,r}\, g_r(t-t_k).$$

If the set of functions $\{g_r(t)\}_{r=0,1,\ldots,R-1}$ is known, the signal $x(t)$ is perfectly determined by the coefficients $(a_{k,r}, t_k)$.

- Let us constrain the input signal to a stream of K Diracs in an interval τ $x(t) = \sum_{k=1}^{K} a_k\, \delta(t-t_k)$, where $t_k \in [0,\tau]$.

Signals with Finite Rate of Innovation (FRI)

- Signals that have a finite number of free parameters

$$x(t) = \sum_{k\in\mathbb{Z}} \sum_{r=0}^{R-1} a_{k,r}\, g_r(t - t_k).$$

If the set of functions $\{g_r(t)\}_{r=0,1,\dots,R-1}$ is known, the signal $x(t)$ is perfectly determined by the coefficients $(a_{k,r}, t_k)$.

- Let us constrain the input signal to a stream of K Diracs in an interval τ $x(t) = \sum_{k=1}^{K} a_k\, \delta(t - t_k)$, where $t_k \in [0, \tau]$.
  - This signal has $2K$ degrees of freedom in a temporal interval τ
  - Local rate of innovation: $\rho = \frac{2K}{\tau}$

Signals with Finite Rate of Innovation (FRI)

- Signals that have a finite number of free parameters

$$x(t) = \sum_{k\in\mathbb{Z}} \sum_{r=0}^{R-1} a_{k,r}\ g_r(t - t_k).$$

If the set of functions $\{g_r(t)\}_{r=0,1,\dots,R-1}$ is known, the signal $x(t)$ is perfectly determined by the coefficients $(a_{k,r}, t_k)$.

- Let us constrain the input signal to a stream of K Diracs in an interval τ $x(t) = \sum_{k=1}^{K} a_k\ \delta(t - t_k)$, where $t_k \in [0, \tau]$.
  - This signal has $2K$ degrees of freedom in a temporal interval τ
  - Local rate of innovation: $\rho = \frac{2K}{\tau}$

- We acquire the signal with a sampling device at regular intervals of time $t = nT$

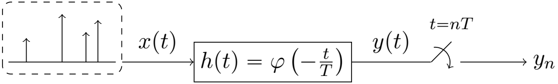

- The output samples can be expressed as $y_n = \langle x(t), \varphi(t/T - n)\rangle$.

$$x(t) = \sum_{k=1}^{K} a_k \, \delta(t - t_k)$$

- Classical sampling theory does not allow to sample and perfectly reconstruct a stream of Diracs because it is not a bandlimited signal.

$$x(t) = \sum_{k=1}^{K} a_k \, \delta(t - t_k)$$

- Classical sampling theory does not allow to sample and perfectly reconstruct a stream of Diracs because it is not a bandlimited signal.

- The FRI framework can achieve perfect reconstruction under some conditions.

$$x(t) = \sum_{k=1}^{K} a_k \, \delta(t - t_k)$$

- Classical sampling theory does not allow to sample and perfectly reconstruct a stream of Diracs because it is not a bandlimited signal.

- The FRI framework can achieve perfect reconstruction under some conditions.

- State of the art FRI algoritms do not deal well with infinite streams:
  - Based on isolating bursts of Diracs
  - Require high sampling rates

$$x(t) = \sum_{k=1}^{K} a_k \, \delta(t - t_k)$$

- Classical sampling theory does not allow to sample and perfectly reconstruct a stream of Diracs because it is not a bandlimited signal.
- The FRI framework can achieve perfect reconstruction under some conditions.
- State of the art FRI algoritms do not deal well with infinite streams:
  - Based on isolating bursts of Diracs
  - Require high sampling rates
- We present a novel sequential algorithm that is able to reconstruct these type of signals:
  - Able to recover 1k Diracs from 10k samples
  - Robust under high noise conditions
  - Works in real time
  - Succesfully applied in neuroscience to infere spiking activity of individual neurons from calcium fluorescence imaging

Sampling process

- We sample $x(t)$ with a very specific kernel: $\varphi(t)$ together with its shifted versions can reproduce exponentials of the form $e^{\alpha_m t}$

$$\sum_{n\in\mathbb{Z}} c_{m,n}\varphi(t-n) = e^{\alpha_m t}, \quad m = 0, 1, \ldots, P$$

Sampling process

- We sample $x(t)$ with a very specific kernel: $\varphi(t)$ together with its shifted versions can reproduce exponentials of the form $e^{\alpha_m t}$

$$\sum_{n\in\mathbb{Z}} c_{m,n}\varphi(t-n) = e^{\alpha_m t}, \quad m = 0, 1, \ldots, P$$

- A family of functions that satisfy the exponential reproducing property are the exponential splines (E-splines). The Fourier transform of the P-th order E-Spline with parameter $\vec{\alpha}_P = (\alpha_0, \alpha_1, \ldots, \alpha_P)$ is given by

$$\hat{\varphi}_{\vec{\alpha}_P}(\omega) = \prod_{m=0}^{P} \left(\frac{1 - e^{\alpha_m - j\omega}}{j\omega - \alpha_m} \right)$$

Sampling process

- We sample $x(t)$ with a very specific kernel: $\varphi(t)$ together with its shifted versions can reproduce exponentials of the form $e^{\alpha_m t}$

$$\sum_{n \in \mathbb{Z}} c_{m,n} \varphi(t-n) = e^{\alpha_m t}, \quad m = 0, 1, \ldots, P$$

- A family of functions that satisfy the exponential reproducing property are the exponential splines (E-splines). The Fourier transform of the P-th order E-Spline with parameter $\vec{\alpha}_P = (\alpha_0, \alpha_1, \ldots, \alpha_P)$ is given by

$$\hat{\varphi}_{\vec{\alpha}_P}(\omega) = \prod_{m=0}^{P} \left(\frac{1 - e^{\alpha_m - j\omega}}{j\omega - \alpha_m} \right)$$

- If coefficients α_m are real, or complex but appear in complex conjugate pairs, the kernel is real valued.
- E-splines present the advantage of being of compact support $P+1$.

Input signal: $x(t) = \sum_{k=1}^{K} a_k \, \delta(t - t_k)$

Samples ($T = 1$): $y_n = \langle x(t), \varphi(t-n) \rangle$

$\varphi(t)$ satisfies: $\sum_{n \in \mathbb{Z}} c_{m,n} \varphi(t-n) = e^{\alpha_m t}, \quad \alpha_m = \alpha_0 + m\lambda$ and $m = 0, \ldots, P$

Input signal: $x(t) = \sum_{k=1}^{K} a_k \, \delta(t - t_k)$

Samples ($T = 1$): $y_n = \langle x(t), \varphi(t-n) \rangle$

$\varphi(t)$ satisfies: $\sum_{n \in \mathbb{Z}} c_{m,n} \varphi(t-n) = e^{\alpha_m t}, \quad \alpha_m = \alpha_0 + m\lambda$ and $m = 0, \ldots, P$

- If we combine samples y_n with coefficients $c_{m,n}$ we obtain a new set of measurements s_m which can be expressed as a sum of exponentials:

$$s_m = \sum_n c_{m,n} \, y_n$$

Input signal: $x(t) = \sum_{k=1}^{K} a_k \, \delta(t - t_k)$

Samples ($T = 1$): $y_n = \langle x(t), \varphi(t-n) \rangle$

$\varphi(t)$ satisfies: $\sum_{n \in \mathbb{Z}} c_{m,n} \varphi(t-n) = e^{\alpha_m t}$, $\alpha_m = \alpha_0 + m\lambda$ and $m = 0, \ldots, P$

- If we combine samples y_n with coefficients $c_{m,n}$ we obtain a new set of measurements s_m which can be expressed as a sum of exponentials:

$$s_m = \sum_n c_{m,n} \, y_n = \sum_{k=1}^{K} \underbrace{a_k \, e^{\alpha_0 t_k}}_{b_k} \left(\underbrace{e^{\lambda t_k}}_{u_k} \right)^m$$

Input signal: $x(t) = \sum_{k=1}^{K} a_k \, \delta(t - t_k)$

Samples ($T = 1$): $y_n = \langle x(t), \varphi(t-n) \rangle$

$\varphi(t)$ satisfies: $\sum_{n \in \mathbb{Z}} c_{m,n} \varphi(t-n) = e^{\alpha_m t}, \quad \alpha_m = \alpha_0 + m\lambda$ and $m = 0, \ldots, P$

- If we combine samples y_n with coefficients $c_{m,n}$ we obtain a new set of measurements s_m which can be expressed as a sum of exponentials:

$$s_m = \sum_n c_{m,n} \, y_n = \sum_{k=1}^{K} \underbrace{a_k \; e^{\alpha_0 t_k}}_{b_k} \left(\underbrace{e^{\lambda t_k}}_{u_k} \right)^m = \sum_{k=1}^{K} b_k \, u_k^m$$

Input signal: $x(t) = \sum_{k=1}^{K} a_k \, \delta(t - t_k)$

Samples ($T = 1$): $y_n = \langle x(t), \varphi(t - n) \rangle$

$\varphi(t)$ satisfies: $\sum_{n \in \mathbb{Z}} c_{m,n} \varphi(t - n) = e^{\alpha_m t}$, $\alpha_m = \alpha_0 + m\lambda$ and $m = 0, \ldots, P$

- If we combine samples y_n with coefficients $c_{m,n}$ we obtain a new set of measurements s_m which can be expressed as a sum of exponentials:

$$s_m = \sum_n c_{m,n} \, y_n = \sum_{k=1}^{K} \underbrace{a_k \, e^{\alpha_0 t_k}}_{b_k} \Big(\underbrace{e^{\lambda t_k}}_{u_k} \Big)^m = \sum_{k=1}^{K} b_k \, u_k^m$$

- Retrieval of a_k and t_k from samples s_m is a classical problem in spectral estimation or in direction of arrival (DOA) estimation
  - Can be solved for instance applying the annihilating filter method (a.k.a. Prony's method) or the matrix pencil method (inspired from ESPRIT)

Input signal: $x(t) = \sum_{k=1}^{K} a_k \, \delta(t - t_k)$

Samples ($T = 1$): $y_n = \langle x(t), \varphi(t-n) \rangle$

$\varphi(t)$ satisfies: $\sum_{n \in \mathbb{Z}} c_{m,n} \varphi(t-n) = e^{\alpha_m t}$, $\alpha_m = \alpha_0 + m\lambda$ and $m = 0, \ldots, P$

- If we combine samples y_n with coefficients $c_{m,n}$ we obtain a new set of measurements s_m which can be expressed as a sum of exponentials:

$$s_m = \sum_n c_{m,n} \, y_n = \sum_{k=1}^{K} \underbrace{a_k \; e^{\alpha_0 t_k}}_{b_k} \left(\underbrace{e^{\lambda t_k}}_{u_k} \right)^m = \sum_{k=1}^{K} b_k \; u_k^m$$

- Retrieval of a_k and t_k from samples s_m is a classical problem in spectral estimation or in direction of arrival (DOA) estimation
  - Can be solved for instance applying the annihilating filter method (a.k.a. Prony's method) or the matrix pencil method (inspired from ESPRIT)

- These methods require a minimum number of values s_m and this in turn imposes a minimal order P for the sampling kernel: $P + 1 \geq 2K$.
  - Critical sampling is achieved for $P + 1 = 2K$

Input signal: $x(t) = \sum_{k=1}^{K} a_k \, \delta(t - t_k)$

Samples ($T = 1$): $y_n = \langle x(t), \varphi(t - n) \rangle$

$\varphi(t)$ satisfies: $\sum_{n \in \mathbb{Z}} c_{m,n} \varphi(t - n) = e^{\alpha_m t}$, $\alpha_m = \alpha_0 + m\lambda$ and $m = 0, \ldots, P$

- If we combine samples y_n with coefficients $c_{m,n}$ we obtain a new set of measurements s_m which can be expressed as a sum of exponentials:

$$s_m = \sum_n c_{m,n} \, y_n = \sum_{k=1}^{K} \underbrace{a_k \, e^{\alpha_0 t_k}}_{b_k} \left(\underbrace{e^{\lambda t_k}}_{u_k} \right)^m = \sum_{k=1}^{K} b_k \, u_k^m$$

- Retrieval of a_k and t_k from samples s_m is a classical problem in spectral estimation or in direction of arrival (DOA) estimation
  - Can be solved for instance applying the annihilating filter method (a.k.a. Prony's method) or the matrix pencil method (inspired from ESPRIT)

- These methods require a minimum number of values s_m and this in turn imposes a minimal order P for the sampling kernel: $P + 1 \geq 2K$.
  - Critical sampling is achieved for $P + 1 = 2K$

- If we have an infinite stream we face some problems:
  - This approach requires knowledge of all samples y_n in order to compute s_m
  - The number of Diracs is infinite so the order of the E-spline must be infinite as well

Sampling an infinite sequence of Diracs

- We consider a continuous time signal $x(t)$ formed by an infinite stream of Diracs, $\sum_{k\in\mathbb{Z}} a_k \, \delta\left(t - t_k\right)$.

Sampling an infinite sequence of Diracs

- We consider a continuous time signal $x(t)$ formed by an infinite stream of Diracs, $\sum_{k\in\mathbb{Z}} a_k\,\delta\,(t-t_k)$.
- There are an infinite number of Diracs, but with a limited rate of at most K Diracs per τ interval.

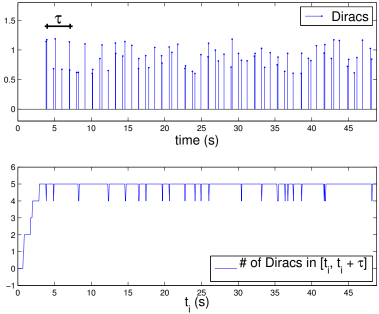

Figure: Infinite stream. Local maximum rate of innovation $\rho = 2K/\tau$ ($K = 5$, $\tau = 3.125$ s).

- We take advantage of the fact that the sampling kernel is of compact support $(P+1)T$. Thus, a Dirac can influence at most $P+1$ samples y_n.

- We take advantage of the fact that the sampling kernel is of compact support $(P+1)T$. Thus, a Dirac can influence at most $P+1$ samples y_n.
- The sequential algorithm estimates the locations of the Diracs within a sliding window that covers the interval of time $\tau = NT$.

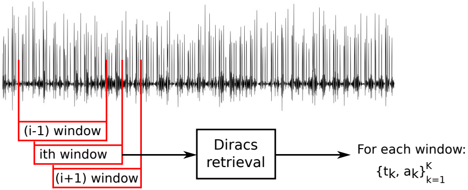

Figure: Sequential processing.

- We take advantage of the fact that the sampling kernel is of compact support $(P+1)T$. Thus, a Dirac can influence at most $P+1$ samples y_n.
- The sequential algorithm estimates the locations of the Diracs within a sliding window that covers the interval of time $\tau = NT$.

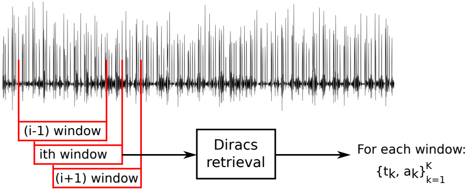

Figure: Sequential processing.

- Problem $\Rightarrow$ if we only process N samples at a time there are border effects when Diracs are located near the borders of the sliding window

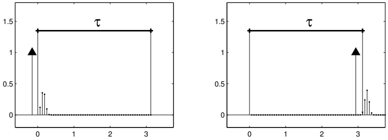

Figure: Border effects.

- The border effect in the left side is due to Dircas before the τ interval that leak into the N samples y_n of the current window.

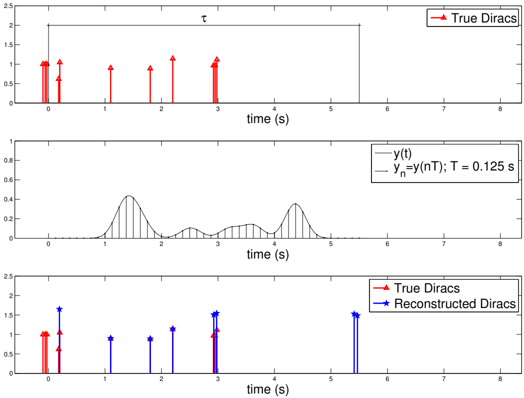

Figure: Diracs are not perfectly recovered because past Diracs corrupt current samples.

- The border effect in the left side is due to Dircas before the τ interval that leak into the N samples y_n of the current window.
- If we assume that we have already recovered Diracs up to the current position of the sliding window we can remove the contribution to y_n of nearby Diracs that happened before.

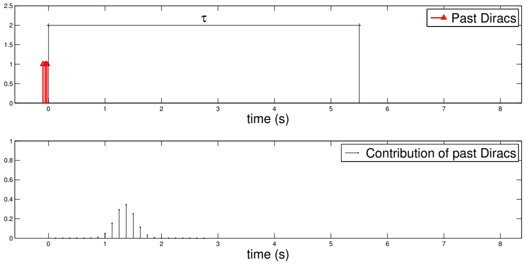

Figure: Contribution of past Diracs to samples y_n.

- The border effect in the left side is due to Dircas before the τ interval that leak into the N samples y_n of the current window.
- If we assume that we have already recovered Diracs up to the current position of the sliding window we can remove the contribution to y_n of nearby Diracs that happened before.

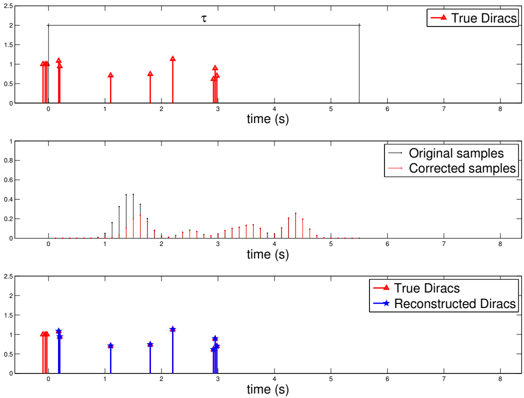

Figure: Perfect reconstruction after correcting past Diracs effect.

- The border effect on the right side is due to Diracs inside the τ interval that leak outside the N samples y_n of the current window.

- The border effect on the right side is due to Diracs inside the τ interval that leak outside the N samples y_n of the current window.
- To make sure that these Diracs will be recovered for a certain position of the sliding window we have to impose:

$$\boxed{T \leq \frac{1}{K\,\rho}} \qquad \text{and} \qquad \boxed{P + 1 = 2K}$$

- The border effect on the right side is due to Diracs inside the τ interval that leak outside the N samples y_n of the current window.
- To make sure that these Diracs will be recovered for a certain position of the sliding window we have to impose:

$$\boxed{T \leq \frac{1}{K\,\rho}} \quad \text{and} \quad \boxed{P+1 = 2K}$$

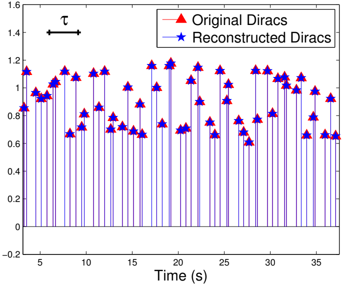

Figure: Sequential perfect reconstruction of a noiseless stream of Diracs. Section of a stream of 1000 Diracs and 10220 samples y_n. Rate $K = 5$ Diracs per $\tau = 3.125$ s, $N = 50$ samples, $T = 1/16$ s and order of the E-spline $P = 9$.

The noisy scenario

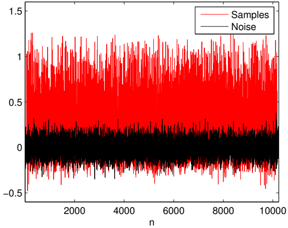

Figure: 1k Diracs, 10k samples, SNR = 10 dB.

- Perfect reconstruction conditions do not hold anymore.
- We can relax conditions on T and P
  - We allow the sampling kernel to be of higher order in order to be more robust against noise.
- The idea is to estimate Diracs by analysing the consistency of the retrieved locations among different positions of the sliding window.

- A Dirac is captured among different positions of the sliding window:
  - If a retrieved location corresponds to a true Dirac this location will be consistent among different positions of the sliding window.

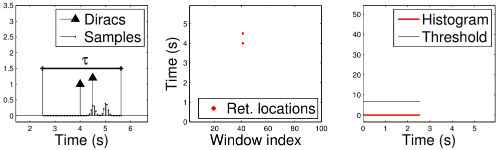

- A Dirac is captured among different positions of the sliding window:
  - If a retrieved location corresponds to a true Dirac this location will be consistent among different positions of the sliding window.

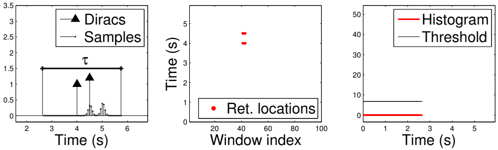

- A Dirac is captured among different positions of the sliding window:
  - If a retrieved location corresponds to a true Dirac this location will be consistent among different positions of the sliding window.

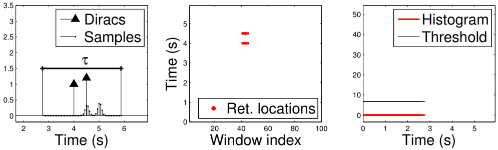

- A Dirac is captured among different positions of the sliding window:
  - If a retrieved location corresponds to a true Dirac this location will be consistent among different positions of the sliding window.

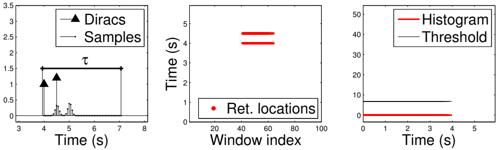

- A Dirac is captured among different positions of the sliding window:
  - If a retrieved location corresponds to a true Dirac this location will be consistent among different positions of the sliding window.

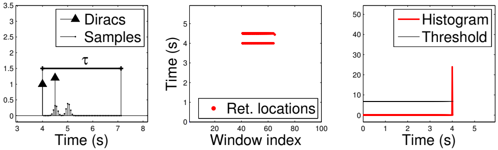

- A Dirac is captured among different positions of the sliding window:
  - If a retrieved location corresponds to a true Dirac this location will be consistent among different positions of the sliding window.

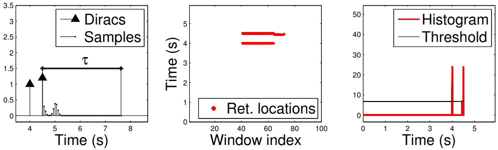

- A Dirac is captured among different positions of the sliding window:
  - If a retrieved location corresponds to a true Dirac this location will be consistent among different positions of the sliding window.

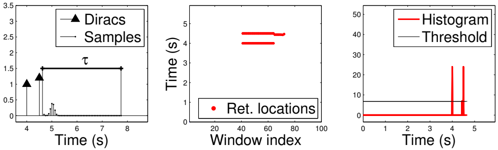

- A Dirac is captured among different positions of the sliding window:
  - If a retrieved location corresponds to a true Dirac this location will be consistent among different positions of the sliding window.

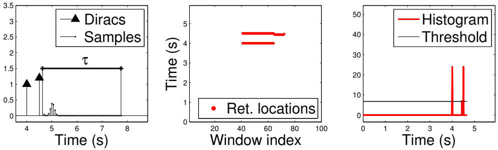

- If we analyse the consistency of the retrieved locations we can estimate the Diracs from the peaks of the histogram of the locations:

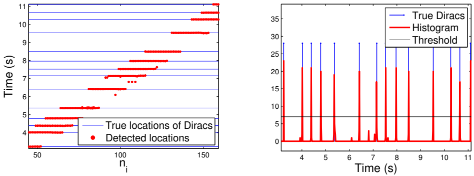

Figure: Retrieved locations among different positions of the sliding window and histogram of locations.

- The consistency analysis makes the retrieval algorithm robust against noise.

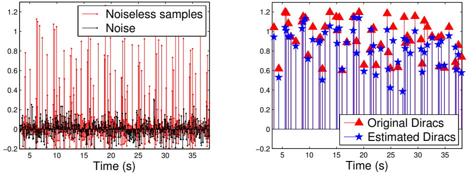

Figure: Sequential reconstruction of a noisy stream of Diracs (SNR = 10 dB). Section of a stream of 1000 Diracs and 10220 samples y_n. Rate $K = 5$ Diracs per $\tau = 3.125$ s, $N = 50$ samples, $T = 1/16$ s and order of the E-spline $P = 22$.

- The consistency analysis makes the retrieval algorithm robust against noise.

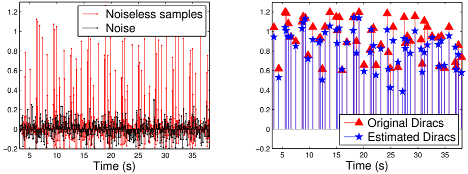

Figure: Sequential reconstruction of a noisy stream of Diracs (SNR = 10 dB). Section of a stream of 1000 Diracs and 10220 samples y_n. Rate $K = 5$ Diracs per $\tau = 3.125$ s, $N = 50$ samples, $T = 1/16$ s and order of the E-spline $P = 22$.

- Some results for differents levels of noise (experiment repeated 100 times for each level of noise):

SNR (dB)	5	10	15	20
Detection rate	97.69 %	99.97 %	100.00 %	100.00 %
False positives	351.7	37.8	0.5	0.3
Precision (s)	0.0086	0.0049	0.0028	0.0018

Application: neural activity detection

- This framework has been successfully applied to the detection of neural activity in calcium concentration movies [1].

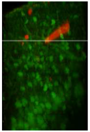

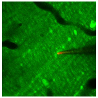

Figure: Simultaneous multiphoton calcium imaging of a region of the cortex and electrophisiological recording of a targeted cell with a micropipette.

[1] Jon Oñativia, Simon R. Schultz and Pier Luigi Dragotti. *A finite rate of innovation algorithm for fast and accurate spike detection from two-photon calcium imaging.* to appear in Journal of Neural Engineering

Application: neural activity detection

- This framework has been successfully applied to the detection of neural activity in calcium concentration movies [1].

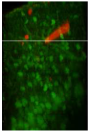
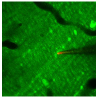

Figure: Simultaneous multiphoton calcium imaging of a region of the cortex and electrophisiological recording of a targeted cell with a micropipette.

- Fluorescence sequences obtained by averaging the pixel values of a ROI can be modeled as a stream of decaying exponentials:

$$c(t) = A \sum_k e^{-\alpha(t-t_k)} u(t - t_k)$$

[1] Jon Oñativia, Simon R. Schultz and Pier Luigi Dragotti. *A finite rate of innovation algorithm for fast and accurate spike detection from two-photon calcium imaging.* to appear in Journal of Neural Engineering

Application: neural activity detection

- This framework has been successfully applied to the detection of neural activity in calcium concentration movies [1].

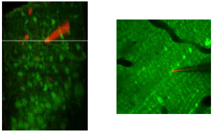

Figure: Simultaneous multiphoton calcium imaging of a region of the cortex and electrophisiological recording of a targeted cell with a micropipette.

- Fluorescence sequences obtained by averaging the pixel values of a ROI can be modeled as a stream of decaying exponentials:

$$c(t) = A \sum_k e^{-\alpha(t-t_k)}\, u(t-t_k) = \underbrace{\sum_k \delta(t-t_k)}_{x(t)} * \underbrace{A\, e^{-\alpha t}\, u(t)}_{\rho_\alpha(t)}$$

[1] Jon Oñativia, Simon R. Schultz and Pier Luigi Dragotti. *A finite rate of innovation algorithm for fast and accurate spike detection from two-photon calcium imaging.* to appear in Journal of Neural Engineering

Application: neural activity detection

- This framework has been successfully applied to the detection of neural activity in calcium concentration movies [1].

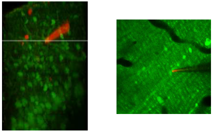

Figure: Simultaneous multiphoton calcium imaging of a region of the cortex and electrophisiological recording of a targeted cell with a micropipette.

- Fluorescence sequences obtained by averaging the pixel values of a ROI can be modeled as a stream of decaying exponentials:

$$c(t) = A \sum_k e^{-\alpha(t-t_k)} u(t-t_k) = \underbrace{\sum_k \delta(t-t_k)}_{x(t)} * \underbrace{A\, e^{-\alpha t} u(t)}_{\rho_\alpha(t)} = x(t) * \rho_\alpha(t).$$

[1] Jon Oñativia, Simon R. Schultz and Pier Luigi Dragotti. *A finite rate of innovation algorithm for fast and accurate spike detection from two-photon calcium imaging.* to appear in Journal of Neural Engineering

Application: neural activity detection

- This framework has been successfully applied to the detection of neural activity in calcium concentration movies [1].

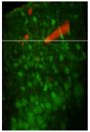
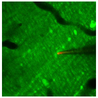

Figure: Simultaneous multiphoton calcium imaging of a region of the cortex and electrophisiological recording of a targeted cell with a micropipette.

- Fluorescence sequences obtained by averaging the pixel values of a ROI can be modeled as a stream of decaying exponentials:

$$c(t) = A\sum_k e^{-\alpha(t-t_k)}\, u(t-t_k) = \underbrace{\sum_k \delta(t-t_k)}_{x(t)} * \underbrace{A\, e^{-\alpha t}\, u(t)}_{\rho_\alpha(t)} = x(t) * \rho_\alpha(t).$$

- This is a Finite Rate of Innovation signal and with a correct processing of the fluorescence samples we can apply our sequential algorithm.

[1] Jon Oñativia, Simon R. Schultz and Pier Luigi Dragotti. *A finite rate of innovation algorithm for fast and accurate spike detection from two-photon calcium imaging.* to appear in Journal of Neural Engineering

- We achieve 84 % detection rates with real data (calcium fluorescence sequence) for electrophysiologically confirmed action potentials.

- We achieve 84 % detection rates with real data (calcium fluorescence sequence) for electrophysiologically confirmed action potentials.
- We outperform state of the art real time spike train inference algorithms:

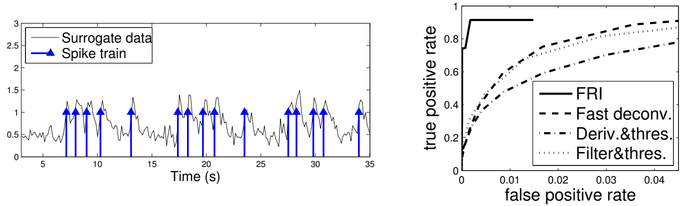

Figure: Receiver operating characteristic (ROC) curves for various algorithms with surrogate data (SNR = 10 dB).

- We achieve 84 % detection rates with real data (calcium fluorescence sequence) for electrophysiologically confirmed action potentials.
- We outperform state of the art real time spike train inference algorithms:

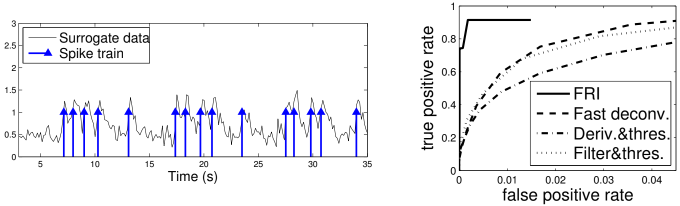

Figure: Receiver operating characteristic (ROC) curves for various algorithms with surrogate data (SNR = 10 dB).

- This technique can be used to monitor tens of neurons simultaneously since the fluorsecence movie captures a volume that contains many neurons.

- We achieve 84 % detection rates with real data (calcium fluorescence sequence) for electrophysiologically confirmed action potentials.
- We outperform state of the art real time spike train inference algorithms:

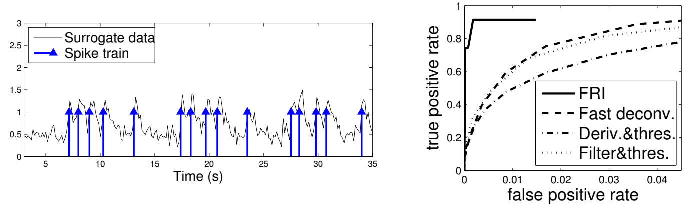

Figure: Receiver operating characteristic (ROC) curves for various algorithms with surrogate data (SNR = 10 dB).

- This technique can be used to monitor tens of neurons simultaneously since the fluorsecence movie captures a volume that contains many neurons.
- The algorithm is fast enough to perform real-time spike inference:
  - The current MATLAB implementation can process more than 80 datastreams in parallel on a commercial laptop (2.5 GHz Intel Core i5 CPU).

Questions?